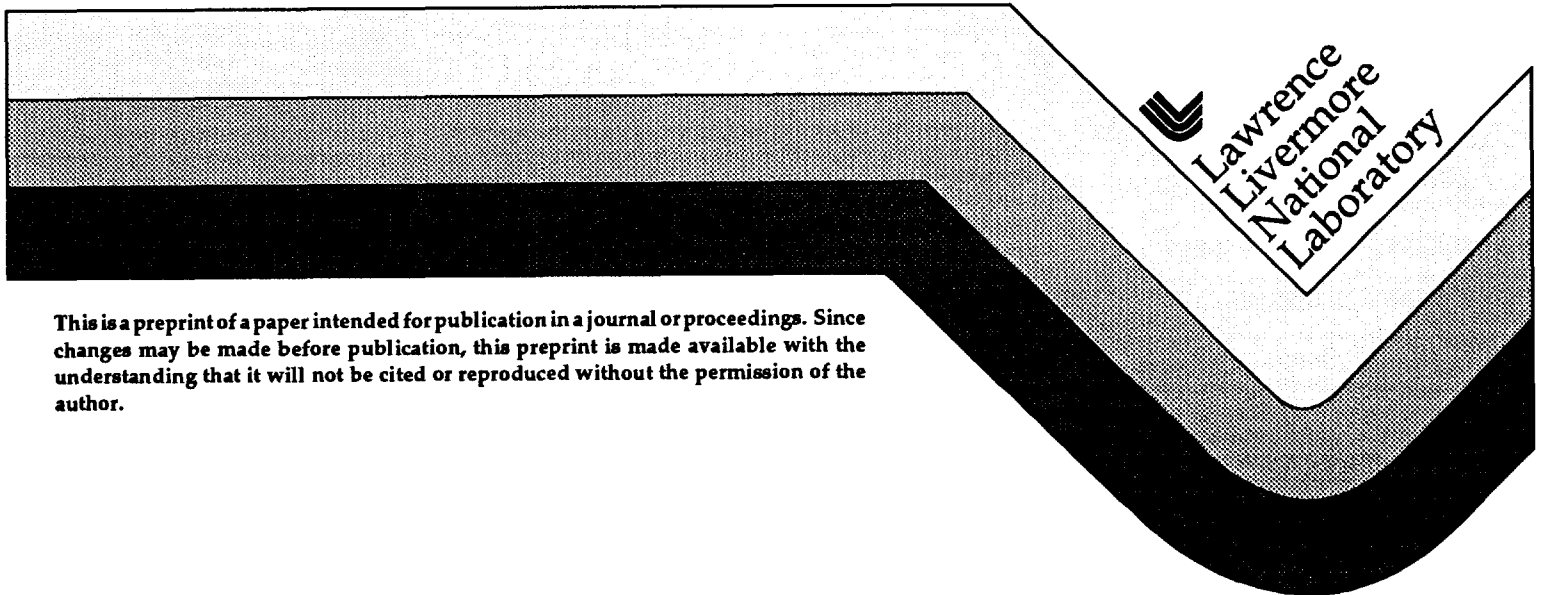


The Impact of Beam Smoothing Method on Direct Drive Target Performance for the NIF

**J. E. Rothenberg
S. V. Weber**

**This paper was prepared for submittal to the
2nd Annual International Conference on
Solid-State Lasers for Application to ICF
Paris, France
October 22-25, 1996**

November 25, 1996



This is a preprint of a paper intended for publication in a journal or proceedings. Since changes may be made before publication, this preprint is made available with the understanding that it will not be cited or reproduced without the permission of the author.

DISCLAIMER

This document was prepared as an account of work sponsored by an agency of the United States Government. Neither the United States Government nor the University of California nor any of their employees, makes any warranty, express or implied, or assumes any legal liability or responsibility for the accuracy, completeness, or usefulness of any information, apparatus, product, or process disclosed, or represents that its use would not infringe privately owned rights. Reference herein to any specific commercial product, process, or service by trade name, trademark, manufacturer, or otherwise, does not necessarily constitute or imply its endorsement, recommendation, or favoring by the United States Government or the University of California. The views and opinions of authors expressed herein do not necessarily state or reflect those of the United States Government or the University of California, and shall not be used for advertising or product endorsement purposes.

The Impact of Beam Smoothing Method on Direct Drive Target Performance for the NIF

Joshua E. Rothenberg and Stephen V. Weber

Lawrence Livermore National Laboratory, L-439

P. O. Box 808, Livermore, CA 94551

Phone: (510) 423-8613, FAX: (510) 422-5537

email: JR1 @ LLNL.GOV

ABSTRACT

The impact of smoothing method on the performance of a direct drive target is modeled and examined in terms of its ℓ -mode spectrum. In particular, two classes of smoothing methods are compared, smoothing by spectral dispersion (SSD) and the induced spatial incoherence (ISI) method. It is found that SSD using sinusoidal phase modulation (FM) results in poor smoothing at low ℓ -modes and therefore inferior target performance at both peak velocity and ignition. Modeling of the hydrodynamic nonlinearity shows that saturation tends to reduce the difference between target performance for the smoothing methods considered. However, using SSD with more generalized phase modulation results in a smoothed spatial spectrum, and therefore target performance, which is identical to that obtained with the ISI or similar method where random phase plates are present in both methods and identical beam divergence is assumed.

Keywords: Beam smoothing, smoothing by spectral dispersion, direct drive, inertial confinement fusion.

1. INTRODUCTION

The laser driver requirements for the successful implementation of direct drive inertial confinement fusion (ICF) are significantly different from those for indirect drive. Direct drive requires a highly uniform illumination pattern on the target in order to minimize imprinted perturbations which are then greatly amplified by Rayleigh-Taylor (RT) growth.¹ The various approaches²⁻⁶ to this uniformity requirement all make use of target illumination with a time varying speckle pattern. The imprint of the high spatial frequencies from speckle on the target is ameliorated by the averaging of multiple uncorrelated speckle patterns over some effective integration time (governed by target physics and generally agreed to less than 1 nsec). Previous beam smoothing analysis has been primarily concerned with aggregate smoothing levels. However, because the target response varies greatly with the spatial frequency of the illuminating nonuniformities, the target performance must be evaluated in terms of the smoothed spatial spectrum. In this paper, an analytic model of the direct drive target response is used to compare the performance of two classes of smoothing methods, smoothing by spectral dispersion (SSD)⁵ and induced spatial incoherence (ISI)².

2. ANALYTIC MODEL

The direct drive inertial confinement fusion implosion can be divided into four regimes: imprint, Rayleigh-Taylor gain during acceleration, stagnation and feed through of external nonuniformities to the inside surface, and Rayleigh-Taylor gain during deceleration. An analytic model of each of these regimes has been developed based on extensive simulations. First we define the angular distribution of the illuminating target fluence by

$$F(\theta, \phi) = \sum_{l,m} Y_{lm}(\theta, \phi) \sqrt{p_{lm}} \quad (1)$$

Assuming degeneracy in m the aggregate variance of the fluence may then be written as a sum over the spectral power in each l -mode

$$\sigma^2 = 1/4\pi \sum_l (2l+1) p_l \quad (2)$$

Simulation of the imprint phase have been approximated by the following analytic description of the efficiency of transfer of fluence nonuniformity to equivalent surface imprint amplitude as a function of l -mode

$$a_{\text{imprint}}(l) = 95 \mu\text{m} \cdot \sqrt{p_l} \exp\left\{- (l/80)^{0.53}\right\} \quad (3)$$

In using this empirical fit to the simulation results, it is assumed that the initial target radius is 1.695 mm. The Rayleigh-Taylor gain each l -mode amplitude experiences during the acceleration is then approximated by the modified Takabe⁷ formula

$$G_{RT}(l) = \exp\left\{ \Delta t \left[\left(\frac{gk}{1+kL} \right)^{1/2} - \beta k v_a \right] \right\} \quad (4)$$

the wave vector $k = l/1 \text{ mm}$, $\beta=3$, $v_a = 3.4 \times 10^5 \text{ cm/s}$, $\Delta t = 4.16 \text{ ns}$, $g = 9 \times 10^{15} \text{ cm/s}^2$, $L = 0.5 \mu\text{m}$. The amplitude at peak velocity is then given by

$$a_{\text{peak-velocity}}(l) = a_{\text{imprint}}(l) \cdot G_{RT}(l) \quad (5)$$

The aggregate variance of the surface perturbation at peak velocity is then given by $\sigma^2 = \sum_l (2l+1) a_{\text{peak-velocity}}^2(l) / 4\pi$. These perturbations then feed through to the surface of the hot core during stagnation according to the approximate amplitude efficiency

$$F_{\text{feed-through}}(l) = (1 + 1/\eta)^{-1} \quad (6)$$

where $\eta=16$.

Finally in the last stage of implosion these perturbations on the core grow during deceleration according to the linear approximation

$$G_{\text{dec}}(l) = 1 + \Delta v k_{\text{dec}} A \Delta t_{\text{dec}}, \quad (7)$$

where $A=0.5$, $\Delta t = 0.2 \text{ ns}$, $\Delta v = 3.8 \times 10^7 \text{ cm/s}$, and $k_{\text{dec}} = l/150 \mu\text{m}$. The surface perturbation of the hot core at ignition is then given by

$$a_{\text{ignition}}(l) = a_{\text{imprint}}(l) \cdot G_{RT}(l) \cdot F_{\text{feed-through}}(l) \cdot G_{\text{dec}}(l). \quad (8)$$

Note that these equations assume unsaturated growth owing to the instabilities. At either peak velocity or ignition one may estimate the effects of nonlinear saturation using the Haan broadband model⁸ when the unsaturated amplitude a_{unsat} is larger than $a_{\text{nl}} = 2R_{\text{sat}}/l^2$. The saturated amplitude is then given by

$$a_{sat}(l) = a_{nl}(l) \left\{ 1 + \ln[a_{unsat}(l) / a_{nl}(l)] \right\} \quad (9)$$

where the compressed target radius R_{sat} is 250 μm at peak velocity and 60 μm at ignition.

3. EFFECT OF THE CHOICE OF SMOOTHING METHOD

Using the above analytic model one can now calculate the target response to a particular smoothing method. The spatial power spectra⁹ (including ℓ -mode degeneracy, is proportional to $(2\ell+1)p_\ell$) of the smoothed fluence for both standard FM-2D-SSD^{5,6} (unless otherwise specified this will be referred to as simply SSD) and modified ISI-type smoothing (hereafter referred to as ISI) are shown approximately in Fig. 1 as a function of the integration times indicated and ℓ -mode. It is of significance to note that the divergence of the method determines the extent of smoothing at low ℓ -mode. In the modified ISI-type method (left, solid curves) it is assumed that a random phase plate (RPP) is present. In this case, the spatial frequencies above the divergence limit (dotted curves, shown for 20, 30, and 50 μrad) are all smoothed equally, whereas below this limit the spatial modes remain unsmoothed. In the ideal ISI method an RPP is absent, the smoothing is equivalent to that with very large divergence and an RPP present, and therefore all spatial frequencies are smoothed equally (continuation with dashed curves). For standard FM-2D-SSD, the smoothed ℓ -mode spectrum is roughly flat over a range which grows from the higher ℓ -modes (solid curves, right of Fig. 1). Thus, SSD offers somewhat better smoothing than ISI at large ℓ -modes, but significantly poorer smoothing at low ℓ -modes. For SSD, just as for modified ISI with an RPP present, there is no smoothing for spatial frequencies below the limit set by the beam divergence. The spectral intensity $S(l)$ shown in Fig. 1 is normalized such that the aggregate variance is given by the simple integral $\sigma^2 = \int S(l) dl / l_{\max}$, where $l_{\max} = 2\pi r_0 D / F\lambda$, corresponds to the $f/\#$ limited maximum speckle ℓ -mode, and the $f/\# = F / D$ is taken to be the NIF value of 20.

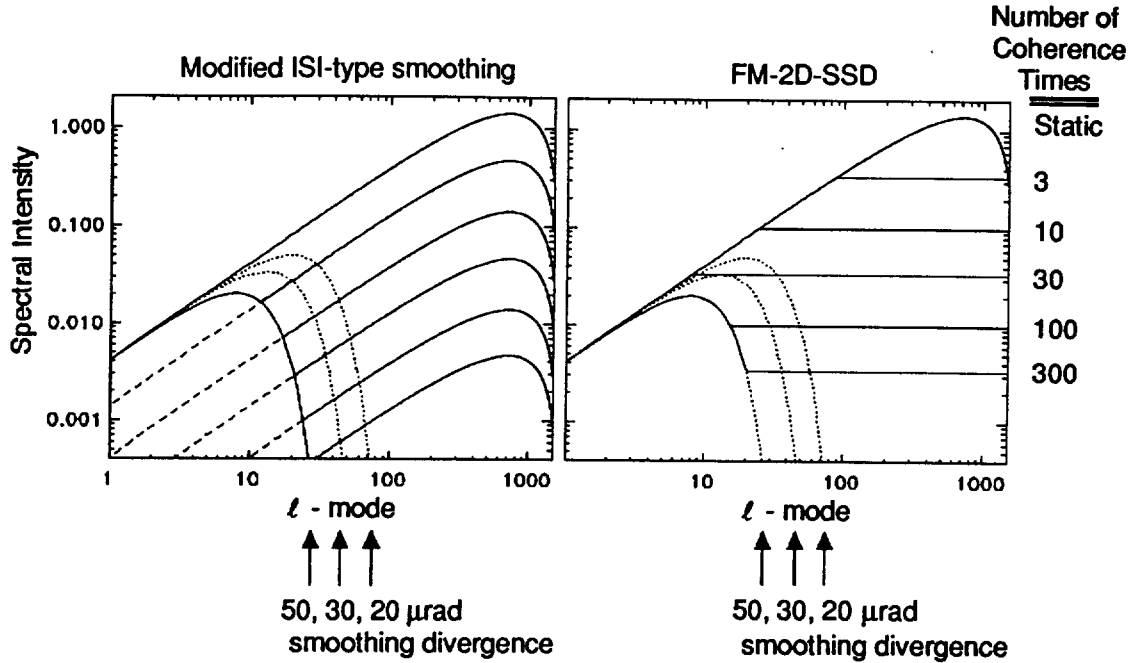


Figure 1: Power spectrum of fluence nonuniformity as a function of the integration times indicated for FM-2D-SSD and modified ISI type smoothing (RPP present, solid curves). Dotted curves show the low ℓ -mode limit of smoothing for three values of induced beam divergence. Ideal ISI (RPP absent, continuing dashed curves) smoothes uniformly for all spatial frequencies.

4. TARGET PERFORMANCE AT PEAK VELOCITY

The effect of the smoothing method at peak velocity is examined in Figs. 2 and 3 (using Eqs. 5 and 9). The solid curve in Fig. 2 shows the unsaturated perturbation amplitude spectrum in the case of 2D SSD and the dashed curve for modified ISI-type smoothing. In these calculations the relevant NIF parameters are assumed: a bandwidth of 500 GHz (coherence time of 2 ps), an effective integration time of 1 ns, effective overlap of 50 beams and two polarizations, and divergence of 50 μrad (with an RPP assumed present in both methods). The results are plotted in RMS per ℓ -mode (i.e. $\sqrt{(2\ell+1)/4\pi} \cdot a_{\text{peak-velocity}}(\ell)$), such that the quadrature sum over ℓ -mode yields the aggregate variance. We estimate that the aggregate RMS perturbation must be less than $\sim 20 \mu\text{m}$ to ensure that the shell maintains integrity through this phase of implosion (the shell thickness here is $\sim 110 \mu\text{m}$). From this calculation it is clear that regardless of smoothing method, the unsaturated amplitudes are too large to maintain shell integrity at peak velocity. In addition, one sees that the amplitudes exceed the nonlinear limit ($a_{nl}(\ell)$, dotted curve) by a factor of ~ 100 for ℓ -modes above 100 (which is where the bulk of the aggregate RMS nonuniformity originates at peak velocity). In Fig. 3 the saturated amplitudes (based on the Haan model as described in Eq. 9) are shown for both smoothing methods. In this figure it is clear that with either smoothing method the saturated amplitudes are below the level required for shell integrity. From this figure one sees that for either saturated or unsaturated amplitudes ISI results in a somewhat more uniform spectrum than SSD.

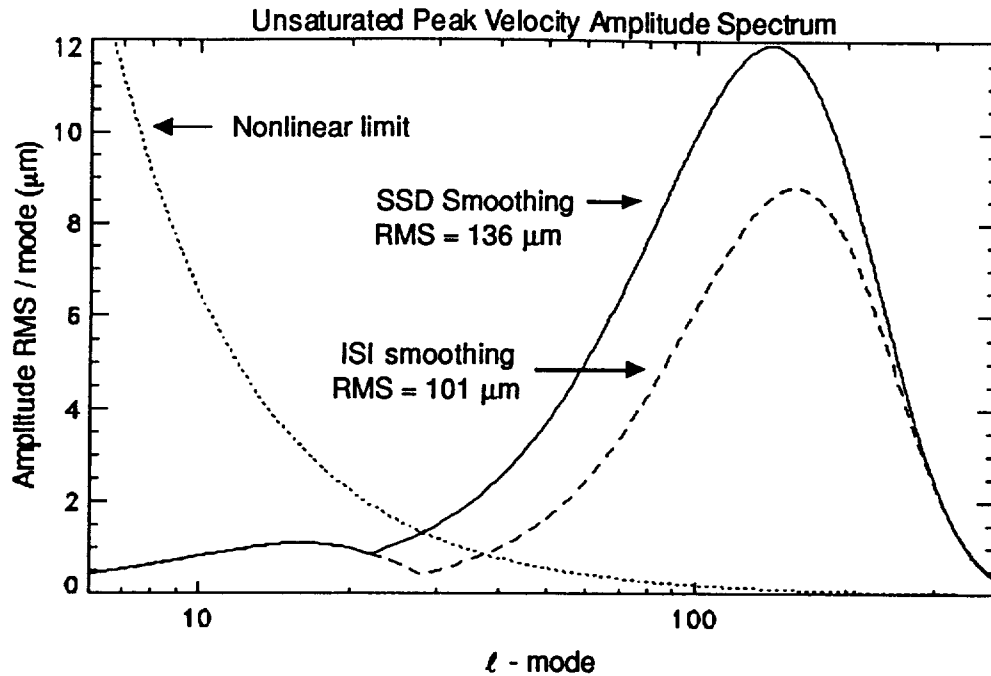


Figure 2: Unsaturated perturbation amplitude at peak velocity for SSD (solid) and ISI (dashed) smoothing methods. The aggregate nonuniformity RMS is indicated for both methods. The nonlinear limit at which saturation becomes significant is shown by the dotted curve.

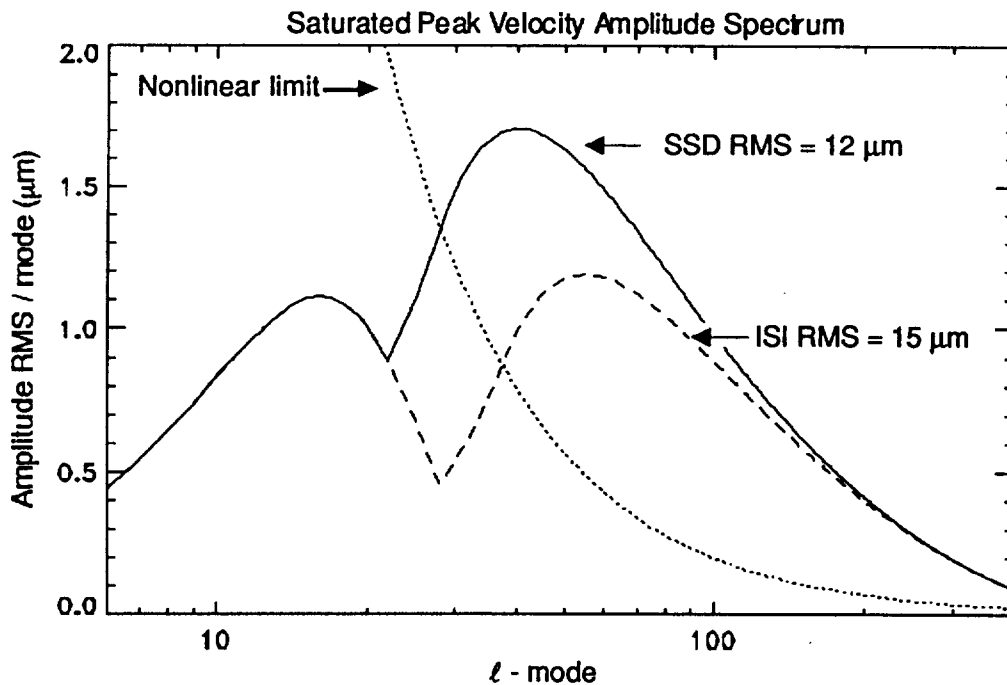


Figure 3: Perturbation amplitude at peak velocity for SSD (solid) and ISI (dashed) smoothing methods, including the effects of nonlinear saturation. The aggregate nonuniformity RMS is indicated for both methods. The nonlinear limit at which saturation becomes significant is shown by the dotted curve.

Since there is significant uncertainty in the duration of the effective integration time of the imprint phase, it is of interest to consider the target performance in terms of this parameter. Fig. 4 shows the aggregate RMS nonuniformity as a function of effective imprint integration time for both saturated and unsaturated amplitudes. In this calculation all other parameters are unchanged: bandwidth of 500 GHz, effective overlap of 50 beams and two polarizations, and divergence of 50 μrad (with an RPP present assumed in both methods) are assumed. From this figure it is apparent that for effective integration times longer than a few hundred picoseconds, the shell integrity is maintained, but only when nonlinear saturation is taken into account. Even though the difference in uniformity is modest at long integration times, it appears that ISI performs significantly better than SSD at short times. For ISI smoothing the 20 mm RMS threshold is crossed at an effective integration time of ~ 30 ps, whereas for SSD the crossing occurs at ~ 170 ps.

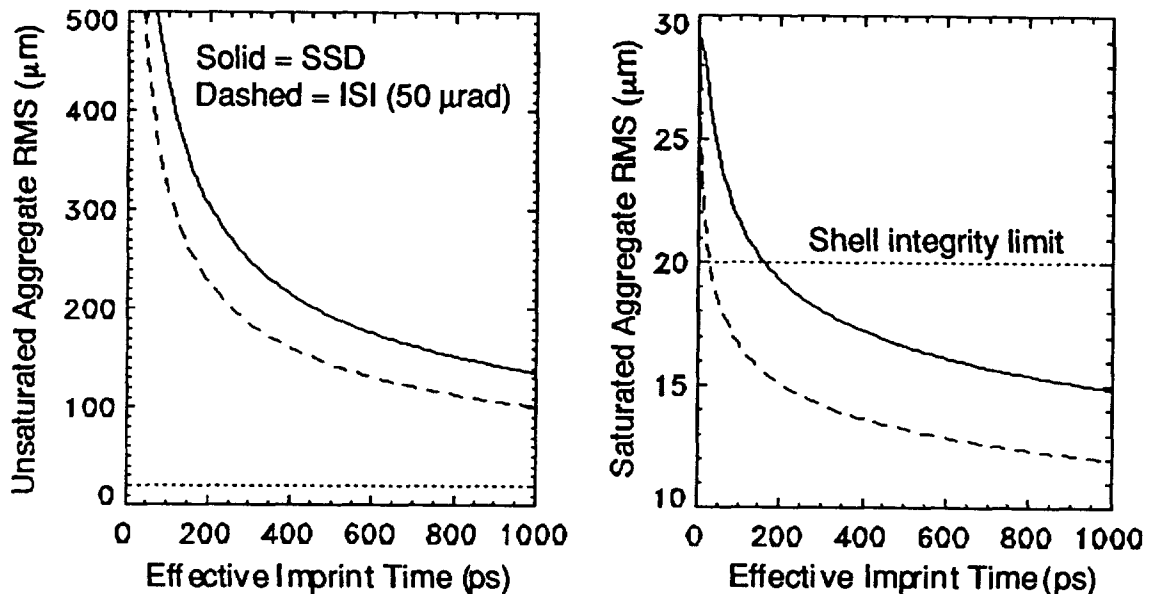


Figure 4: Aggregate RMS perturbation amplitude at peak velocity for SSD (solid) and ISI (dashed) smoothing methods versus the effective imprint integration time of the target, without (left) and including the effects of nonlinear saturation (right). The estimated maximum perturbation allowed to maintain shell integrity is ~ 20 μm and shown by a dotted line.

5. TARGET PERFORMANCE AT IGNITION

Figures 5 and 6 show the effect of SSD (solid curve) and ISI (dashed curve) on the unsaturated and saturated amplitude spectra, respectively, of the core perturbations at the time of ignition (using Eqs. 8 and 9). The core radius at ignition is ~ 60 mm and the maximum allowable RMS core mix is estimated to be ~ 10 mm. In the unsaturated spectrum one sees a fairly significant difference between the results for SSD and ISI-type smoothing.

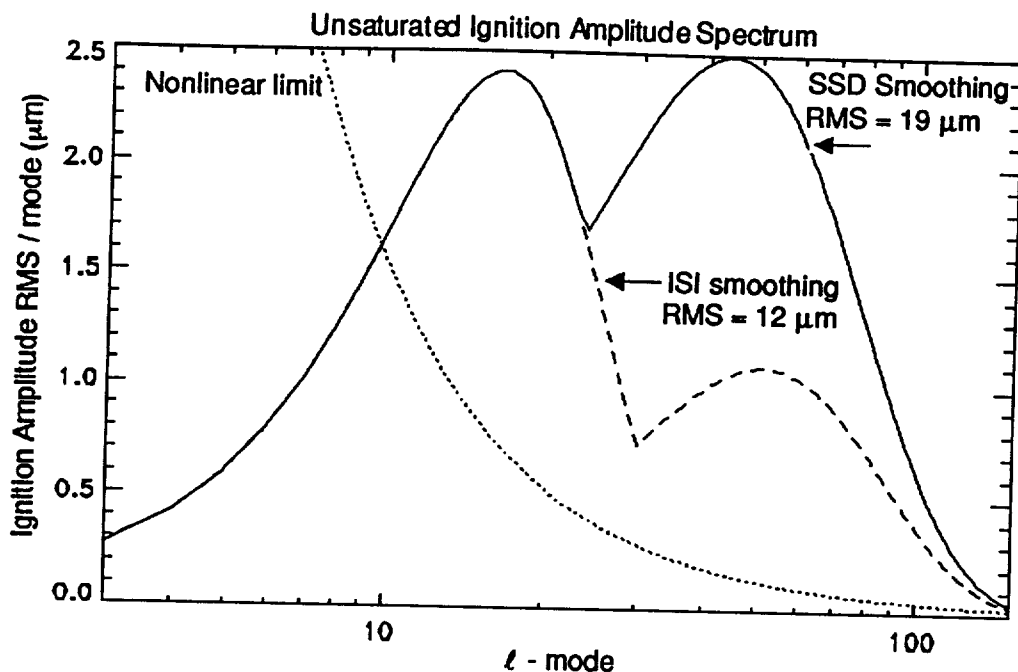


Figure 5: Unsaturated perturbation amplitude at ignition for SSD (solid) and ISI (dashed) smoothing methods. The aggregate nonuniformity RMS is indicated for both methods. The nonlinear limit at which saturation becomes significant is shown by the dotted curve.

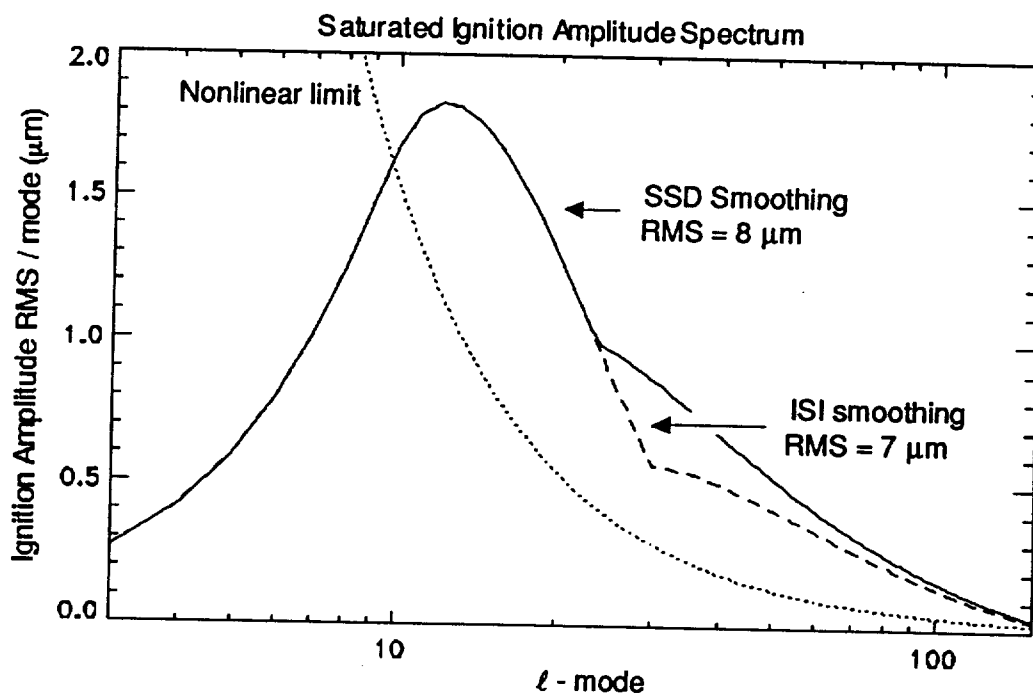


Figure 6: Perturbation amplitude at ignition for SSD (solid) and ISI (dashed) smoothing methods, including the effects of nonlinear saturation. The aggregate nonuniformity RMS is indicated for both methods. The nonlinear limit at which saturation becomes significant is shown by the dotted curve.

Although not so highly saturated as in the case of peak velocity, it is clear that the presence of nonlinear saturation improves the target performance significantly at ignition as well. However, with the effects of saturation included, one sees that the difference between SSD and modified ISI-type smoothing is quite small.

From these figures it is also apparent that the unsmoothed low ℓ -mode lobe of the spectrum contributes significantly to the aggregate RMS nonuniformity at ignition. Therefore, the aggregate RMS level will be strongly dependent on the extent of the low ℓ -mode smoothing and hence on the amount of smoothing divergence. This behavior is shown in Fig. 7, where the aggregate RMS level is shown as function of effective imprint integration time for modified ISI-type smoothing at various levels of divergence and ideal ISI. For either the saturated or unsaturated spectrum it is clear that the divergence of the smoothing plays an important role. Note however, that for modified ISI-type smoothing with a divergence of $\sim 100 \mu\text{rad}$, the aggregate RMS is nearly identical to that of ideal ISI (i.e. ISI of very large divergence or without an RPP present).

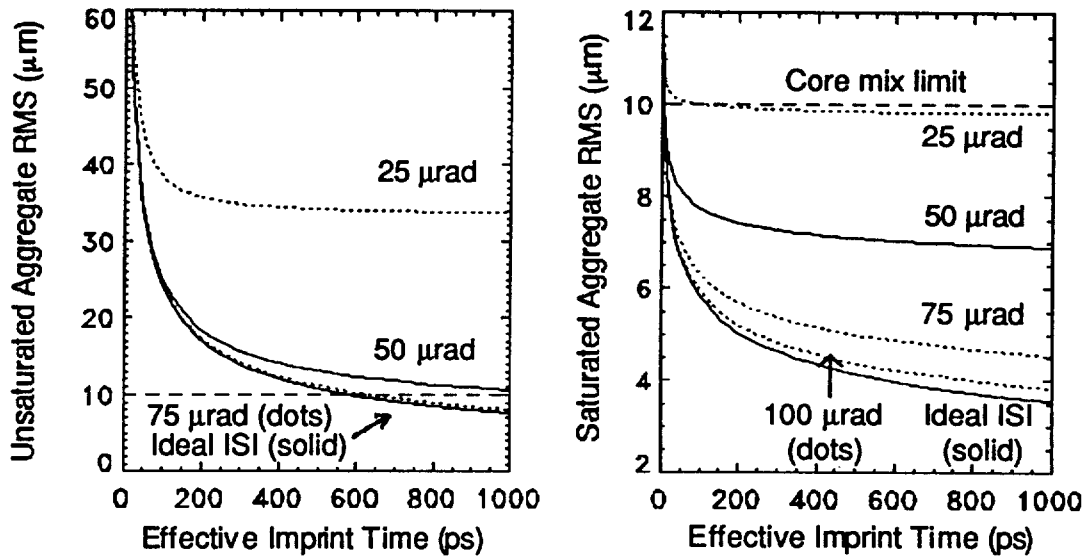


Figure 7: Aggregate RMS perturbation amplitude at ignition for the ISI smoothing method (solid and dotted curves) versus the effective imprint integration time of the target and for the amounts of beam divergence indicated, without (left) and including the effects of nonlinear saturation (right). The result for ideal ISI (without an RPP or with very large divergence) is also shown as indicated. The estimated maximum of core mix allowed to maintain ignition is $\sim 10 \mu\text{m}$ and shown by a dashed line.

In all the above analysis it was assumed that 2D SSD was used with the usual sinusoidal FM. However, since it has been shown that 2D SSD with advanced phase modulation (such as random phase modulation or multiple FM) achieves smoothing spectra equivalent to that of modified ISI-type smoothing with equivalent bandwidth and divergence,⁹ one can conclude

that such advanced SSD of divergence $\sim 100 \mu\text{rad}$ will yield target performance equal to that of ideal ISI.

6. CONCLUSIONS

Based on the analytic implosion model presented, it has been shown that at peak velocity, with either SSD or modified ISI-type smoothing, the shell surface nonuniformity is ~ 100 times larger than the nonlinear limit. Using the Haan model of nonlinear saturation, one finds that the shell integrity is maintained if the effective time over which the imprint is integrated is longer than a few hundred picoseconds. At peak velocity, although both SSD and ISI smoothing produce similar asymptotic target uniformity, ISI results in much better uniformity at early times. At ignition, the assumption of nonlinear saturation is again required for optimal target performance. With saturation included in the model, ISI and SSD have very similar performance when equal divergence is assumed. The divergence associated with either smoothing method is critical to determining the performance at low ℓ -modes. For a divergence of $\sim 100 \mu\text{rad}$ the target performance with modified ISI-type smoothing is equivalent to that of ideal ISI (without an RPP present). In all the above cases, 2D SSD using advanced phase modulation, such as random phase modulation or multiple FM in series can achieve target performance equivalent to that of modified ISI-type of equal divergence, or of ideal ISI when the SSD divergence is $\sim 100 \mu\text{rad}$.

7. ACKNOWLEDGMENT

This work was performed under the auspices of the U. S. Department of Energy by Lawrence Livermore National Laboratory under Contract No. W-7405-Eng-48.

8. REFERENCES

1. J. D. Kilkenny, S. G. Glendinning, S. W. Haan, B. A. Hammel, J. D. Lindl, D. Munro, B. A. Remington, S. V. Weber, J. P. Knauer, and C. P. Verdon, "A review of the ablative stabilization of the Rayleigh-Taylor instability in regimes relevant to inertial confinement fusion," *Phys. Plasmas* **1**, 1379-1389 (1994).
2. R. H. Lehmberg and S. P. Obenshain, "Use of induced spatial incoherence for uniform illumination of laser fusion targets," *Optics Comm.* **46**, 27-31 (1983) and R. H. Lehmberg and J. Goldhar, "Use of incoherence to produce smooth and controllable irradiation profiles with KrF fusion lasers," *Fusion Technology* **11**, 532-541 (1987).
3. Y. Kato, K. Mima, N. Miyanaga, S. Arinaga, Y. Kitagawa, M. Naktsuka, and C. Yamanka, "Random phasing of high-power lasers for uniform target acceleration and plasma instability suppression," *Phys. Rev. Lett.* **53**, 1057-1060 (1984).
4. D. Véron, H. Ayrat, C. Gouedard, D. Husson, J. Lauriou, O. Martin, B. Meyer, M. Rostaing, and C. Sauteret, "Optical spatial smoothing of Nd-glass laser beam," *Optics Comm.* **65**, 42-45 (1988).
5. S. Skupsky, R. W. Short, T. Kessler, R. S. Craxton, S. Letzring, and J. M. Soures, "Improved laser-beam uniformity using the angular dispersion of frequency-modulated light," *J. Appl. Phys.* **66**, 3456-3462 (1989).

6. J. E. Rothenberg, "Two dimensional beam smoothing by spectral dispersion for direct drive inertial confinement fusion," Proc. Soc. Photo-Opt. Instrum. Eng. 2633, 634-644 (1995).
7. M. Tabak, D. H. Munro, and J. D. Lindl, "Hydrodynamic stability and the direct drive approach to laser fusion", Phys. Fluids B 2, 1007-1014 (1990).
8. S. W. Haan, "Onset of nonlinear saturation for Rayleigh-Taylor growth in the presence of a full spectrum of modes", Phys. Rev. A 39, 5812-5825 (1989).
9. J. E. Rothenberg, "Improved Beam Smoothing with SSD using Generalized Phase Modulation" paper P35 in these proceedings.